Non-Blazhko RR Lyrae stars observed with the KEPLER space telescope

Carnegie Observatories Astrophysics Series, Vol. 5:
RR Lyrae Stars, Metal-Poor Stars, and the Galaxy
ed. A. McWilliam (Pasadena: Carnegie Observatories)

Non-Blazhko RR Lyrae Stars Observed with the KEPLER Space Telescope

J.M. Nemec[1,2], R. Smolec[3], J. M. Benkő[4], P. Moskalik[5], K. Kolenberg[3,6], R. Szabó[4], D. W. Kurtz[7], S. Bryson[8], E. Guggenberger[3], M. Chadid[9], Y.-B. Jeon[10], A. Kunder[12], A. C. Layden[13], K. Kinemuchi[8], L. L. Kiss[4], E. Poretti[14], J. Christensen-Dalsgaard[11], H. Kjeldsen[11], D. Caldwell[15], V. Ripepi[16], A. Derekas[4], J. Nuspl[4], F. Mullally[15], S. E. Thompson[15], W. J. Borucki[8]

(1) Department of Physics & Astronomy, Camosun College, Victoria, BC, Canada;
(2) International Statistics & Research Corporation, PO Box 39, Brentwood Bay, BC, Canada;
(3) Institut für Astronomie, University of Vienna, Türkenschanzstrasse 17, A-1180 Vienna, Austria;
(4) Konkoly Obs.Hung.Acad.Sciences, Konkoly Thege Miklós út 15-17, H-1121 Budapest, Hungary;
(5) Copernicus Astronomical Center, ul. Bartycka 18, 00-716 Warsaw, Poland;
(6) Harvard College Observatory, 60 Garden Street, Cambridge, MA 02138, USA;
(7) Jeremiah Horrocks Institute of Astrophysics, Univ. Central Lancashire, Preston PR1 2HE, UK;
(8) NASA Ames Research Center, MS 244-30, Moffett Field, CA 94035, USA;
(9) Obs. Côte d'Azur, Univ.Nice Sophia-Antipolis, UMR 6525, Parc Valrose, France;
(10) Korea Astronomy and Space Science Institute, Daejeon, 305-348, Korea;
(11) Department of Physics and Astronomy, Aarhus University, DK-8000 Aarhus C, Denmark;
(12) Cerro Tololo Inter-American Observatory, Cassila 603, La Serena, Chile;
(13) Physics & Astronomy Dept., Bowling Green State University, Bowling Green, Ohio OH 43403;
(14) Osservatorio Astronomico di Brera, Via E. Bianchi 46, 23807 Merate, Italy;
(15) SETI Institute/NASA Ames Research Center, MS 244-30, Moffett Field, CA 94025, USA;
(16) INAF-Osservatorio Astronomico di Capodimonte, Via Moiariello 16, I-80131, Napoli, Italy.

Abstract

This paper summarizes the main results of our recent study of the non-Blazhko RR Lyrae stars observed with the *Kepler* space telescope. These stars offer the opportunity for studying the stability of the pulsations of RR Lyrae stars and for providing a reference against which the Blazhko RR Lyrae stars can be compared. Of particular interest is the stationarity of the low-dispersion ($\sigma < 1$mmag) light curves constructed from ∼18000 long-cadence (30-min) and (for FN Lyr and AW Dra) the ∼150000 short-cadence (1-min) photometric data points. Fourier-based [Fe/H] values and other physical characteristics are also derived. When the observed periods are compared with periods computed with the Warsaw non-linear convective pulsation code better agreement is achieved assuming *pulsational* L and $\mathcal{M}$ values rather than the (higher) *evolutionary*

L and $\mathcal{M}$ values.

1. Introduction

In the 105 deg^2 field of the *Kepler* space telescope there are ∼40 RR Lyr stars brighter than 17th magnitude being observed at both long and short cadence (*i.e.*, integrated exposure times of ∼30-min and 1-min, respectively). With the notable exception of RR Lyrae itself (Kolenberg *et al.* 2010, 2011) little was known about the stars prior to the launch of telescope. Several of the RR Lyrae stars are c-type stars pulsating in the first overtone mode (Moskalik *et al.* 2011, in preparation). The remainder are ab-type stars pulsating in the fundamental mode, approximately half of which exhibit the Blazhko effect (see Benkő *et al.* 2010) and show phase and amplitude variations of the light curves occurring on time scales of ∼10 to hundreds of days. The other half of the RRab stars appear to oscillate in a remarkably constant manner and are the subject of our recent paper "Fourier analysis of non-Blazhko ab-type RR Lyrae stars observed with the *Kepler* space telescope" (Nemec *et al.* 2011), the results of which are summarized here. Elsewhere in these conference proceedings Kinemuchi (2011) reviews the general properties of the *Kepler* RR Lyrae star observations, and Kolenberg (2011) discusses the Blazhko RR Lyrae stars.

After deriving pulsation periods, times of maximum light, and total amplitudes, and characterising the light curves using Fourier decomposition methods, attention is turned to [Fe/H] values and how the stars compare with other RR Lyrae stars in our Galaxy and in the Large Magellanic Cloud. After establishing that there are systematic offsets between the V and Kp Fourier parameters, the Kp versions of the correlations established by Kovács, Jurcsik, Walker, Sandage and others are used to derive physical characteristics for the stars. These include the dereddened colour $(B-V)_0$, mean effective temperature, $T_{\rm eff}$, surface gravity, log g, and pulsational and evolutionary luminosities (L) and masses ($\mathcal{M}$). Finally, the results are compared with new theoretical model results computed with the Warsaw non-linear hydrodynamics code.

2. Observations and Data Analysis

For each of the 19 stars listed in **Table 1** the *Kepler* raw-flux data acquired over the first 420 days of the telescope's operation (Q0-Q5) was analysed. The mean apparent magnitudes of the stars (from the *Kepler* Input Catalog) range from $\langle Kp \rangle = 12.7$ to 17.4 mag, with distances ∼3-23 Kpc in the direction $(l, b) = (76.3°, 13.5°)$. The last two columns of Table 1 identify the particular *Kepler* data that was analyzed.

Figure 1 shows the raw-flux (left panel) and fully-transformed Kp-magnitude (right panel) as a function of time for one of the non-Blazhko stars, V894 Cyg (graphs such as these are typical). The flux is in units of e^-/s/cadence ($\log_{10}$ scale) and 18911 long cadence (LC) aperture photometry measurements are plotted. Since the 1.4-m

TABLE 1
Non-Blazhko ab-type RR Lyrae stars in the *Kepler* field:
Pulsation Periods, Times of Maximum Light, and Analyzed Data

Star Name	KIC Number	$\langle Kp \rangle$ [mag]	Period [day]	t_0 [BJD]	Kepler data	No. Pts.
NR Lyr	3733346	12.683	0.6820264(2)	54964.7381	LC:Q1-Q5	18333
V715 Cyg	3866709	16.265	0.47070494(4)	54964.6037	LC:Q1-Q5	18374
V782 Cyg	5299596	15.392	0.5236377(1)	54964.5059	LC:Q1-Q5	18381
V784 Cyg	6070714	15.370	0.5340941(1)	54964.8067	LC:Q1-Q5	18364
KIC 6100702	6100702	13.458	0.4881457(2)	54953.8399	LC:Q0-Q4	14404
NQ Lyr	6763132	13.075	0.5877887(1)	54954.0702	LC:Q0-Q5	18759
FN Lyr	6936115	12.876	0.52739845(1)	54953.2690	SC:Q0+Q5	149925
	-	-	0.527398471(4)	54953.2690	LC:Q1-Q5	18338
KIC 7021124	7021124	13.550	0.6224926(7)	54965.6471	LC:Q1	1595
KIC 7030715	7030715	13.452	0.6836137(2)	54953.8434	LC:Q0-Q5	18802
V349 Lyr	7176080	17.433	0.5070740(2)	54964.9555	LC:Q1-Q5	18314
V368 Lyr	7742534	16.002	0.4564851(1)	54964.7828	LC:Q1-Q5	18273
V1510 Cyg	7988343	14.494	0.5811436(1)	54964.6695	LC:Q1-Q5	18394
V346 Lyr	8344381	16.421	0.5768281(1)	54964.9211	LC:Q1-Q5	18362
V350 Lyr	9508655	15.696	0.5942369(1)	54964.7795	LC:Q1-Q5	18326
V894 Cyg	9591503	13.293	0.5713866(2)	54953.5627	LC:Q1-Q5	18362
V2470 Cyg	9947026	13.300	0.5485894(1)	54953.7808	LC:Q0-Q5	18794
V1107 Cyg	10136240	15.648	0.5657781(1)	54964.7532	LC:Q1-Q5	18373
V838 Cyg	10789273	13.770	0.4802799(1)	54964.5731	LC:Q1-Q5	18241
AW Dra	11802860	13.053	0.6872158(6)	54954.2160	SC:Q0	14240
	-	-	0.687217(1)	54954.2160	LC:Q1	1614
	-	-	0.6872158(2)	54954.2160	LC:Q5	4474
	-	-	0.68721632(3)	54954.2160	SC:Q5	135380

telescope was rolled by 90° every three months resulting in a given star being observed with different pixels every 'quarter', it was necessary to correct for sensitivity variations from quarter to quarter, and for drift within each quarter. The Kp magnitudes were derived from the fully normalized and detrended photometry. The scalloped pattern seen at maximum and minimum light, and the moiré pattern seen everywhere, result from the pulsation period for this star, 0.571 d, not being evenly divisible by the LC sampling period, ∼30 min, giving rise to 27 observations per pulsation cycle. The constancy of the range in the total amplitude is remarkable, as is the continuous moiré pattern.

The pulsation period for each star (fundamental mode) was derived from the high-precision aperture photometry using the PERIOD04 period-finding program (Lenz & Breger 2005) and a version of the CLEAN program written by Dr. Seung-Lee Kim (see Nemec, Walker & Jeon 2009). Typically the LC data consisted of ∼18000 points, and the short cadence (SC) observations of FN Lyr and AW Dra (Q0 and Q5) amounted to another ∼150000 data points per star. The uncertainties in the derived periods are

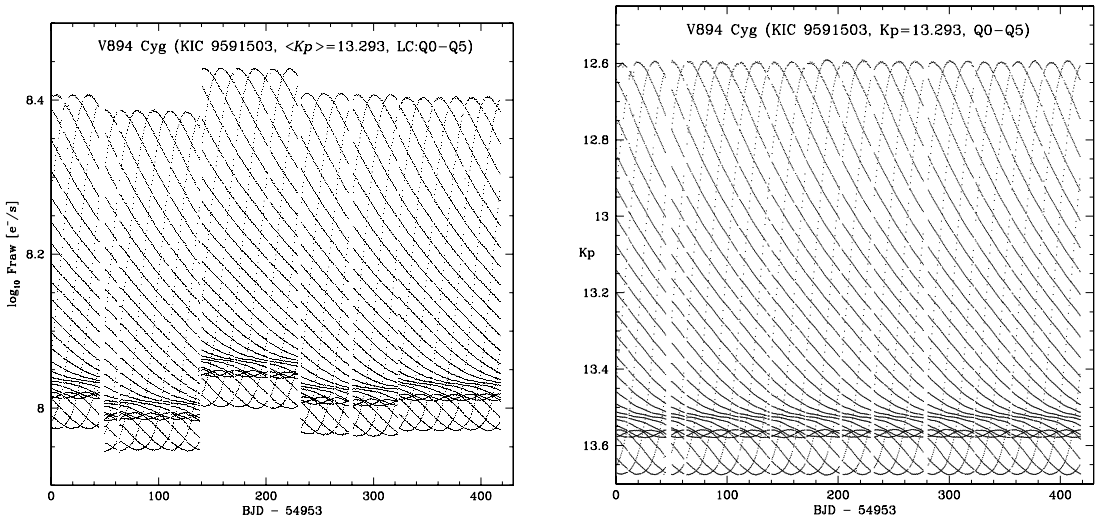

Figure 1.— Raw-flux (left) and Kp-magnitude (right) long-cadence photometry for V894 Cyg, one of the 19 non-Blazhko RR Lyrae stars in the *Kepler* field. The processing of the raw-flux data consisted of normalizing the different (Q0-Q5) sensitivities, removing (minor) trending within each quarter, stitching together the quarters, and shifting the magnitudes to $\langle Kp \rangle = 13.293$ mag. The times are BJD (Barycentric Julian Date) minus 54953.0 (the first day of *Kepler* observations).

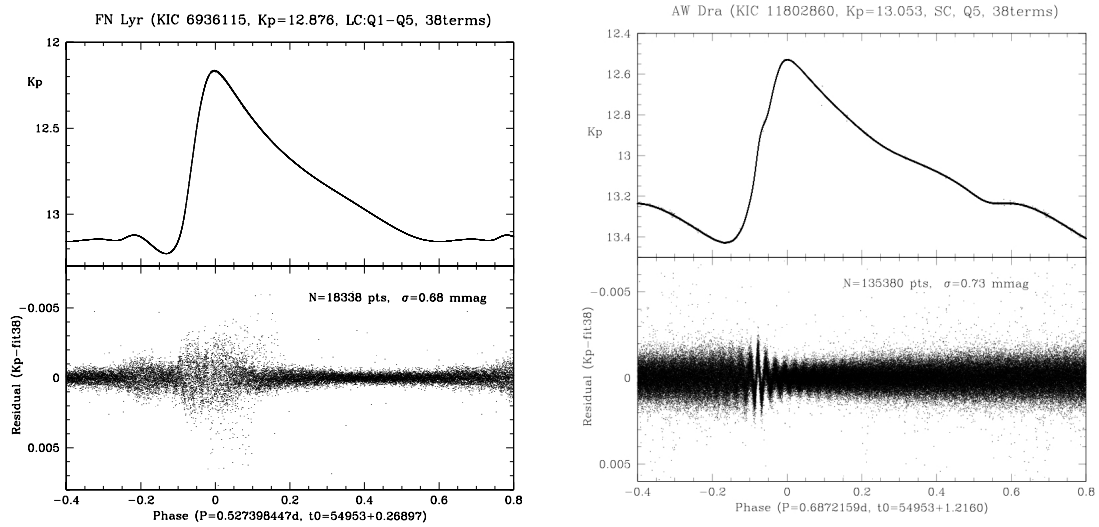

Figure 2.— (Left) Light curve for FN Lyr derived from Q1-Q5 long-cadence photometry; (Right) Light curve for AW Dra derived from short-cadence Q5 photometry. (Lower) The residual plots in both cases are from the 38-term Fourier fits (observed minus fitted). The standard deviations of the fits in both cases are below 1 mmag and would be even smaller with more terms in the Fourier fit.

$\sim$1-2$\times10^7$d, depending on the particular data set and pulsation period, P. Times of maximum light, t_0, accurate to $\pm$0.0005 d also were computed. The P and t_0 values are summarized in columns 4 and 5 of Table 1.

Phased light curves for all 19 non-Blazhko stars were plotted using the derived pulsation periods and times of maximum light. Two such light curves are illustrated in the top panels of **Figure 2**. The light curve for FN Lyr is based on 18338 LC data points acquired over ∼400 days in Q1-Q5, and that on the right is for AW Dra and is based on 135380 SC data points acquired over 90 days in Q5. When the light curves for all the stars are plotted one clearly sees variations in the 'risetimes' (*i.e.*, the time from minimum to maximum light, expressed in phase units), the stars with the shortest risetimes having the largest amplitudes and a tendency to have a bump on the rise to maximum light.

Also analyzed were new high precision ground-based V photometry for three of the stars (NR Lyr, FN Lyr and AW Dra), and All Sky Automated Survey (ASAS) V, I photometry (see Pigulski *et al.* 2009) for nine of the brightest stars. The high-precision calculations were instrumental in establishing the V-Kp offsets in the Fourier parameters (needed to permit use of the Kovács, Jurcsik *et al.* relations); and the ASAS-North data (http://www.astrouw.edu.pl/asas/kepler), although not providing high-precision Fourier parameters, were sufficient for deriving reliable loop diagrams in the HR-diagram, from which it is clear that in every case the non-Blazhko stars are bluest when brightest (as expected).

By combining the historical data (going back more than 100 years for FN Lyr, NQ Lyr and AW Dra) with the *Kepler* data we were also able to derive period change rates for some of the stars. In particular, the periods for FN Lyr and AW Dra were seen to be increasing. Unfortunately the baseline of the *Kepler* observations is still too short to derive significant period variations directly.

Finally, one of the non-Blazhko stars, KIC 7021124, was discovered to be doubly-periodic and to have properties very similar to V350 Lyr (Benkő *et al.* 2010). Both appear to be pulsating in the fundamental and second-overtone modes simultaneously. The period ratios are almost identical, $P_2/P_0 = 0.59305$ for KIC 7021124, and 0.592 for V350 Lyr. When masses are derived for these two stars using the Petersen P_2/P_0 vs. P_0 diagram the best agreement with the models is obtained, in both cases, for a high luminosity and a high mass: $L/L_\odot = 70$ and $\mathcal{M}/\mathcal{M}_\odot = 0.75$.

3. Fourier Analysis

Fourier decomposition of the light curves was performed on the fully calibrated photometry for all the stars by fitting the following Fourier series to the apparent magnitudes:

$$m(t) = A_0 + \sum_{i=1}^{F} A_i \sin[2\pi i f_0(t - t_0) + \phi_i], \tag{1}$$

where $m(t)$ is the apparent magnitude (either Kp for the *Kepler* data, or m_V for the ground based V-photometry), F is the number of fitted terms, f_0 is the (assumed

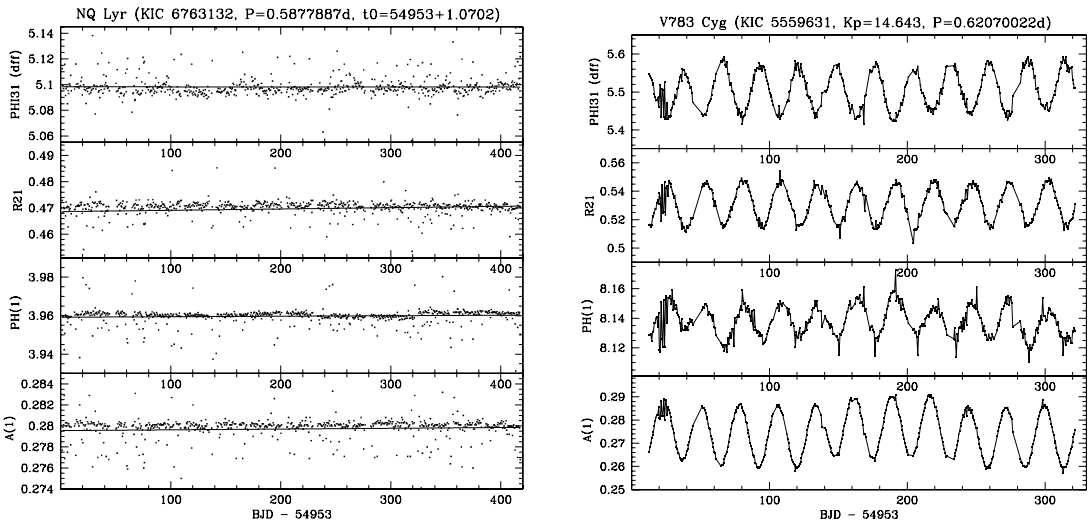

Figure 3.— Variations in time of the Fourier parameters PHI31, R21, PHI1S and A1 derived for the typical non-Blazhko star NQ Lyr (left panel) and for the known low-amplitude Blazhko star V783 Cyg (right panel). Each point corresponds to the variable of interest as determined from a single pulsation cycle.

single) pulsation frequency of the star ($=P_0^{-1}$), t is the observed time of the observation (BJD-54953 for the *Kepler* data), t_0 is the time of maximum light used to phase the light curves (so that maximum light occurs at zero phase), and the A_i and ϕ_i are the amplitude and phase coefficients for the individual Fourier terms. The Fourier calculations were made with two FORTRAN programs, one kindly provided by Dr. Géza Kovács, and the other by Dr. Pawel Moskalik. The assumed pulsation periods were those derived either from the *Kepler* data or from the period change rate analysis, and the t_0 values were calculated numerically.

The Fourier analyses were performed on various subsets of the data. The bottom panels of Fig.2 show residual plots after fitting 38-term Fourier descriptions to all the data. In both cases the standard deviations about the mean curve are below 1 mmag, specifically ∼60 μmagn, and the greatest differences occur where the slope is steepest. For the purposes of using extant Fourier correlations to derive physical characteristics only the lower order Fourier terms are needed. Owing to the small risetimes as many as 100 or more terms could be needed for a normal distribution of the residuals.

Another way of looking at the data was to calculate Fourier coefficients and parameters for each pulsation cycle. For the long cadence (30 min) data there were ∼24 observations per bin for an RRab star with a period of 12 hours, and fewer (more) observations per cycle for stars with shorter (longer) periods. None of the 19 stars exhibits the recently discovered "period doubling" effect, thus confirming the result found earlier by Szabó *et al.* (2010). For the Fourier calculations 'direct Fourier fitting' (dff) rather than 'template Fourier fitting' (tff) methods were used (see Kovács & Kupi 2007), and for each star the resulting time series were plotted for four Fourier parame-

ters: A_1, the first term in the Fourier series (see right panel of Fig. 2); ϕ_1, the phase of the first term; R_{21}, the amplitude ratio A_2/A_1; and ϕ^s_{31}, the Fourier parameter found by Simon, Kovács and others to be one of the most significant variables for deriving physical characteristics. Typical time series are illustrated in **Figure 3**, on the left for the unmodulated RRab star NQ Lyr having intermediate amplitude (A_1=0.279 mag) and intermediate brightness, $\langle Kp \rangle = 13.075$ mag, and on the right for V783 Cyg, a low-amplitude Blazhko star with the shortest Blazhko period ($P_B = 27.7 \pm 0.04$ d) among the stars in the sample. For NQ Lyr linear trend lines were fit to each time series and in almost every case the slope is zero to within the systematic and random uncertainties. The mean values for the four parameters are as follows: $\phi^s_{31} = 5.0958 \pm 0.0023$, with residual standard error, $\sigma = 0.002$; $R_{21} = 0.4710 \pm 0.0006$, with $\sigma = 0.0006$; $\phi^s_1 = 3.961 \pm 0.001$, with $\sigma = 0.001$; and $A_1 = 0.28016 \pm 0.00014$ mag, with $\sigma = 0.0001$. Since the other non-Blazhko stars show random variations of the Fourier parameters similar to those shown here for NQ Lyr these means and errors provide a measure of the typical uncertainties. Inspection of the NQ Lyr time series in Fig. 3 shows that the stability over the ∼420 d interval (Q0-Q5) is exceptional, not only for each Fourier parameter but for the ensemble of parameters. To better illustrate the remarkable stationarity of the light curves for all 19 sample stars a set of 'animated gif' light curves was prepared and these are available in the electronic version of the MNRAS paper.

In **Table 2** some of the resulting Fourier coefficients and parameters are summarized. Column 2 gives the standard deviation about the mean light curve (see Fig.2), most of which are below one mmag. Column 3 contains the first term in the Fourier series, which correlates extremely well with the total amplitude. Columns 4 and 5 contain amplitude ratios (defined above) and columns 6 and 7 contain phase parameters (see Simon 1988 and references therein).

It is of interest to compare the derived Fourier parameters for the 19 non-Blazhko stars in the *Kepler* field (derived using the *Kp* photometry but transformed to *V* values using the offsets) with parameters derived for Galactic globular clusters and for RR Lyrae stars in the Large Magellanic Cloud.

Figure 4 compares the non-Blazhko stars with 177 RR Lyr stars in several well-studied globular clusters (from Kovács & Walker 2001). The same symbols and colour coding are used in all four panels. The **upper-left** panel is analogous to the P-$A_{\rm tot}$ diagram (see Fig.6 below) and was used to derive [Fe/H] values for the *Kepler* stars. The two diagonal lines represent mean relations when the globular cluster data (small black dots) are sorted into two [Fe/H] bins (the 'BB' subscript refers to the Butler-Blanco system, which approximates the Carretta-Gratton system): a metal-poor bin consisting of 19 stars (surrounded by blue squares) with metallicities between −1.70 and −1.99 dex and average −1.8 dex (BB-scale); and an intermediate-metallicity bin consisting of 39 stars (circled in red) with $[{\rm Fe/H}]_{\rm BB}$ between −0.97 and −1.23 dex and average −1.1 dex. The equations of the lines are: $\phi^c_{31} = 5.556 \log P + 0.2920$ (upper metal-poor bin) and $\phi^c_{31} = 6.200 \log P + 3.615$ (lower intermediate metallicity bin). Four of the *Kepler* non-Blazhko stars are clearly richer than $[{\rm Fe/H}]_{\rm BB}$=−1.1 dex, while the

TABLE 2
Selected Fourier Parameters and Derived Metallicities for the *Kepler* non-Blazhko ab-type RR Lyrae stars

Star	σ [mmag]	A_1 [mag]	R_{21}	R_{31}	ϕ^s_{21} [rad]	ϕ^s_{31} [rad]	[Fe/H]$_{ZW}$
NR Lyr	0.69	0.266	0.456	0.352	2.416	5.115	-2.34
V715 Cyg	1.74	0.338	0.479	0.358	2.314	4.901	-1.44
V782 Cyg	0.79	0.190	0.488	0.279	2.777	5.808	-0.47
V784 Cyg	0.96	0.234	0.487	0.253	2.904	6.084	-0.14
KIC 6100702	0.66	0.209	0.493	0.279	2.743	5.747	-0.35
NQ Lyr	0.65	0.280	0.471	0.356	2.389	5.096	-1.83
FN Lyr	0.64	0.380	0.444	0.350	2.322	4.818	-1.90
KIC 7021124	1.10	0.283	0.512	0.351	2.372	5.060	-2.08
KIC 7030715	0.71	0.231	0.494	0.303	2.683	5.606	-1.66
V349 Lyr	3.24	0.346	0.450	0.352	2.328	4.845	-1.73
V368 Lyr	1.57	0.405	0.464	0.341	2.272	4.784	-1.53
V1510 Cyg	0.82	0.345	0.473	0.355	2.389	5.068	-1.83
V346 Lyr	2.83	0.330	0.473	0.352	2.372	5.060	-1.83
V350 Lyr	1.67	0.340	0.485	0.342	2.389	5.124	-1.84
V894 Cyg	0.91	0.377	0.490	0.338	2.364	5.067	-1.79
V2470 Cyg	0.79	0.220	0.488	0.282	2.745	5.737	-0.71
V1107 Cyg	0.99	0.280	0.495	0.350	2.421	5.196	-1.56
V838 Cyg	1.22	0.393	0.465	0.349	2.300	4.853	-1.56
AW Dra	0.55	0.306	0.525	0.346	2.730	5.560	-1.74

remainder are apparently more metal poor. The **upper-right** panel of Fig. 4 shows that the *Kepler* stars appear to be drawn from a distribution similar to that of the globular clusters. In particular, the *Kepler* stars with low R_{31} values are not unusual, except possibly that they all have relatively high R_{21} values. Since the globular cluster stars of higher metallicity (red open circles) all tend to reside on the right side of the diagram this separation is probably a metallicity effect, supporting our conclusion that V784 Cyg, V782 Cyg, KIC 6100702 and V2470 Cyg are metal rich. Likewise, the **lower-left** panel shows that the majority of the *Kepler* stars do not differ from the stars in globular clusters. Note too that there is very little metallicity discrimination in this plane. The two stars located at the extreme upper edge of the envelope of the globular cluster distribution are AW Dra and V784 Cyg. Finally, the **lower-right** panel shows close agreement between the phase parameters of the *Kepler* and globular cluster RR Lyr stars, which supports the conclusion drawn earlier (lower-right panel in Fig. 4) that there is a strong approximately-linear correlation between ϕ^s_{21} and ϕ^s_{31}. The diagram also shows very little dependence on metallicity.

Figure 5 compares the R_{21}, R_{31}, ϕ^c_{21} and ϕ^c_{31} Fourier parameters for the 19 *Kepler* non-Blazhko RR Lyr stars with those for the field RR Lyr stars in the central regions of the LMC. The LMC data are from the massive OGLE-III catalog of variable stars

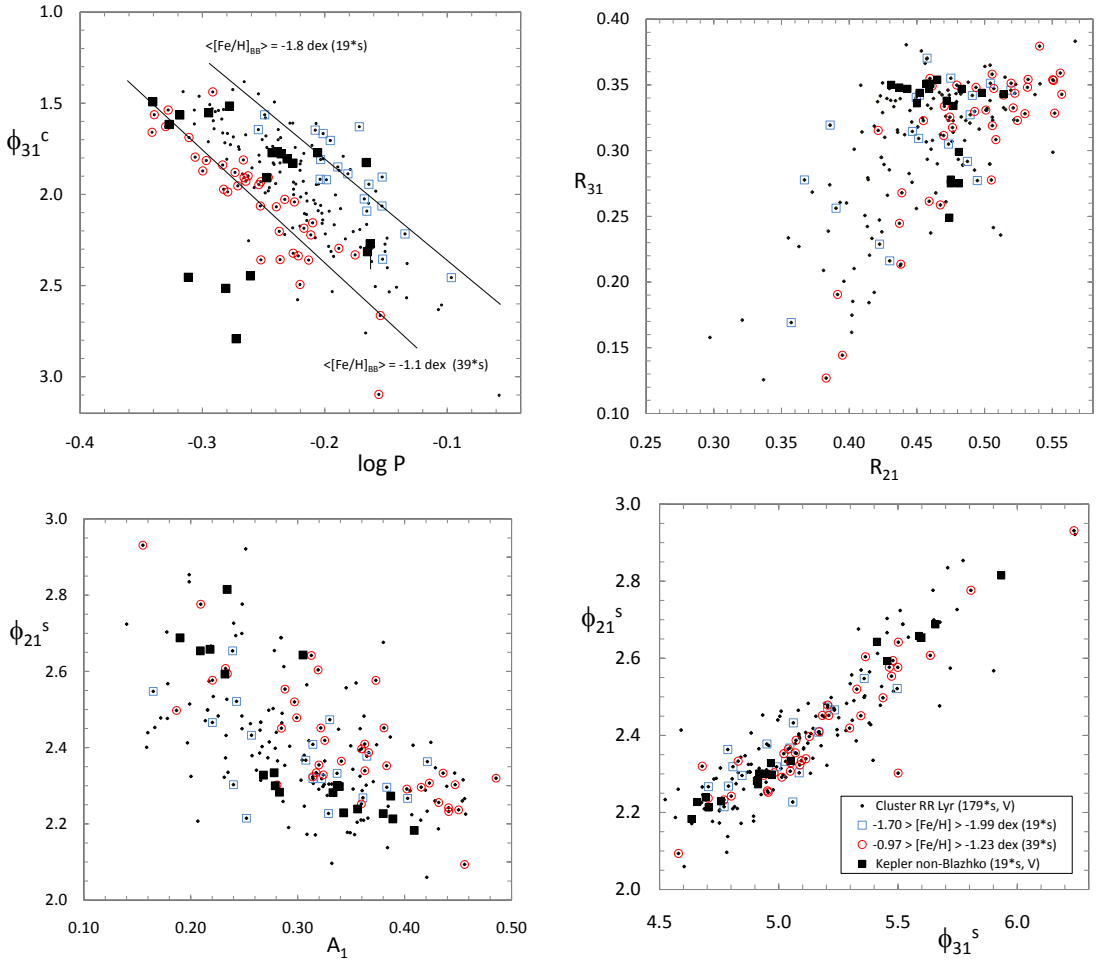

Figure 4.— Four panels comparing the Fourier parameters (transformed to the V-band) for the *Kepler* non-Blazhko stars (large black squares) and for the 177 RR Lyr stars located in several Galactic and LMC globular clusters (small black dots). The cluster RR Lyr stars (from Kovács & Walker 2001) are in the globular clusters M2 (12 stars), M4 (4), M5 (12), M55 (4), M68 (5), M92 (5), NGC 1851 (11), NGC 5466 (6), NGC 6362 (12), NGC 6981 (20), IC 4499 (49), Ruprecht 106 (12), NGC 1466 (8), Reticulum (8) and NGC 1841 (9). The points for the 19 most metal-poor globular cluster stars are surrounded by blue squares, and the points for the 39 most metal-rich globular cluster stars are circled in red.

by Soszynski *et al.* (2009), which comprises almost 25000 RR Lyr stars. All the parameters are V-band values, the LMC values having been transformed from I to V using the transformation equations given by Morgan, Simet & Bargenquast (1998), and the values for the *Kepler* RR Lyr stars transformed from Kp to V using the well-determined offsets from diagrams such as Fig.6 below. The **upper-left** panel shows that the R_{21} values for the *Kepler* stars are typical for ab-type RR Lyr stars and they all lie in the narrow range 0.45 to 0.51. The period ranges of the RRab stars also are similar. Where the LMC stars differ from the *Kepler* stars is in the much larger R_{21} range; in particular, none of the *Kepler* stars are among the LMC stars in the

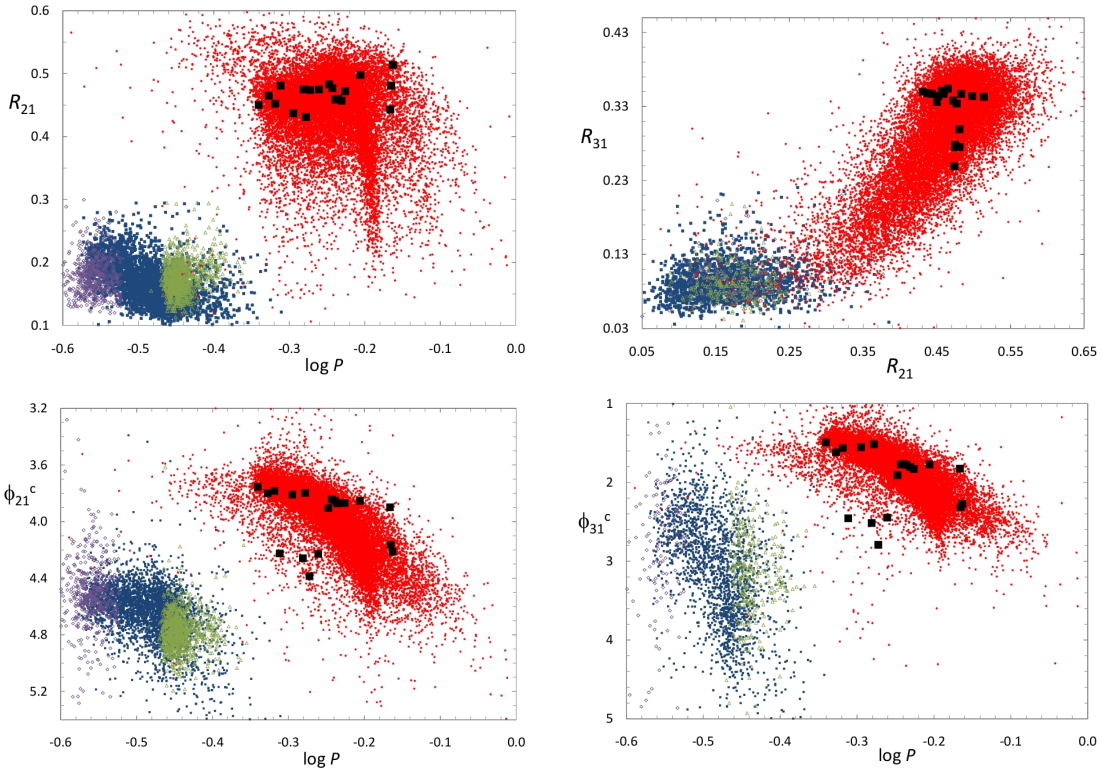

Figure 5.— Four panels comparing Fourier parameters (V-band) for the *Kepler* non-Blazhko ab-type RR Lyr stars (large black squares) and for 24905 RR Lyr stars in the central regions of the Large Magellanic Cloud. The LMC data are from the Soszynski *et al.* (2009) OGLE-III study, with colour and symbol coding as follows: red filled dots (17693 RRab stars); blue filled squares (4957 RRc stars); green open triangles (986 RRd stars), and purple open diamonds (1269 RRe stars). Because of the limited x- and y-ranges not all of the LMC RR Lyr stars are represented in the graphs.

'dropdown' at log$P \sim -0.19$. It is suspected that the majority of these are RRab Blazhko variables. In the **upper-right** panel of Fig. 5 the R_{21} and R_{31} amplitude ratios are compared. This graph puts into perspective the small ranges of R_{21} and R_{31} seen for the *Kepler* non-Blazhko RRab stars, both relative to that for the LMC RRab stars, and relative to the ranges seen for other types of RR Lyr stars (RRc, RRd and RRe). The upper left panel of Fig. 4 has already shown that the *Kepler* stars sort into four metal-rich and 15 metal-poor stars, and that the metal-poor stars are similar to the RR Lyr stars found in Galactic globular clusters (both OoI and OoII types); however, the metal-rich stars have no counterparts, at least among the Kovács & Walker (2001) sample of globular cluster RR Lyr stars. In the **bottom** panels of Fig. 5 (both of which are metallicity diagnostics) we see that both the metal-rich *Kepler* RR Lyr stars (the clump of four stars at log$P \sim -0.3$ and $\phi^c_{21} \sim 4.3$) and the metal-poor *Kepler* RR Lyr stars (the majority with lower ϕ^c_{21} values) have counterparts in the LMC, and that the metal-rich stars appear to have relatively long periods for metal-rich RRab stars (*i.e.*, the subgroup of RRab stars with shorter periods at a given ϕ^c_{31}).

4. Physical Characteristics based on Fourier Parameters

Several different physical characteristics were established using equations derived by Jurcsik (1998, hereafter J98), Kovács & Walker (2001), and Sandage (2004, 2006). Since these equations were originally established for V data, and we have only Kp data, it was necessary first to establish Kp versions of the equations. The specific equations used to derive the physical quantities, and the detailed tables given in Nemec *et al.* (2011) are not repeated here, but the results of their application are summarized in several graphs and discussed below.

Figure 6 shows four different metallicity diagnostic diagrams. The upper-left panel is the classical period-amplitude diagram, often called the 'Bailey P-A diagram' but coined the 'Oosterhoff-Arp-Preston P-A diagram' by Sandage (2004, hereafter S04). At a given total-amplitude lower [Fe/H] stars tend to have longer periods. Spectroscopically calibrated diagonal lines, such as that shown in the lower right panel for the Messier 3 RRab stars ($\phi_{31}^c = 3.124 + 5.128 \log P$), can be constructed, from which offsets give [Fe/H] values. Since the pattern of the stars seen in all four panels is very similar all four variables can, in principle, be used to derive [Fe/H] values. Four different estimates of [Fe/H] were calculated by Nemec *et al.* (2011), based on the ϕ_{31}^s relation of J98 (her equation 1), the ϕ_{31}^c relation of S04 (his equation 3), the $A_{\rm tot}$ relation of S04 (his equation 6), and the 'risetime' relation of S04 (his equation 7). The ϕ_{31} relations seem to be the most reliable and the [Fe/H] values based on the J98 formula, after conversion to the Zinn-West scale, are given in the last column of Table 2. Recently acquired CFHT 3.6-m ESPaDOnS spectra confirm that KIC 6100702 is indeed metal-rich, at [Fe/H] = -0.18±0.06 dex, while AW Dra is of intermediate metallicity, with [Fe/H] = -1.33±0.08 (Nemec, Ripepi, Chadid *et al.* 2011, in preparation).

Figure 7 summarizes the derived de-reddened colour information in the form of correlation diagrams. In all four panels the four more metal rich stars stand apart from the more metal-poor stars. For this reason they have been plotted with open squares. The linear correlations show that the reddest metal-poor stars (those nearest the red edge of the Instability Strip) are more metal poor, have longer periods and smaller total amplitudes, and are more luminous than the bluest metal-poor stars. The diagrams also show that at a given colour the four metal-rich stars (plotted with open squares) have shorter periods, smaller amplitudes and are less luminous than the metal-poor stars.

Not represented in these diagrams but computed and given in the full paper are absolute magnitudes (V-passband), surface gravities, mean effective temperatures, distances, and luminosities and masses. Both pulsational and evolutionary L and $\mathcal{M}$ values were computed. The L(puls) were calculated using equations 16 and 17 of J98, and in both cases the lower metallicity stars have the higher L(puls). The $\mathcal{M}$(puls) were calculated using equations 14 and 22 of J98. The average mass for the four metal-rich stars is $\sim$0.50 $\mathcal{M}_\odot$ compared with the average mass for the more metal-poor stars $\sim$0.60 $\mathcal{M}_\odot$. Three different L(evol) were calculated, using equations 8, 10 and 12 of

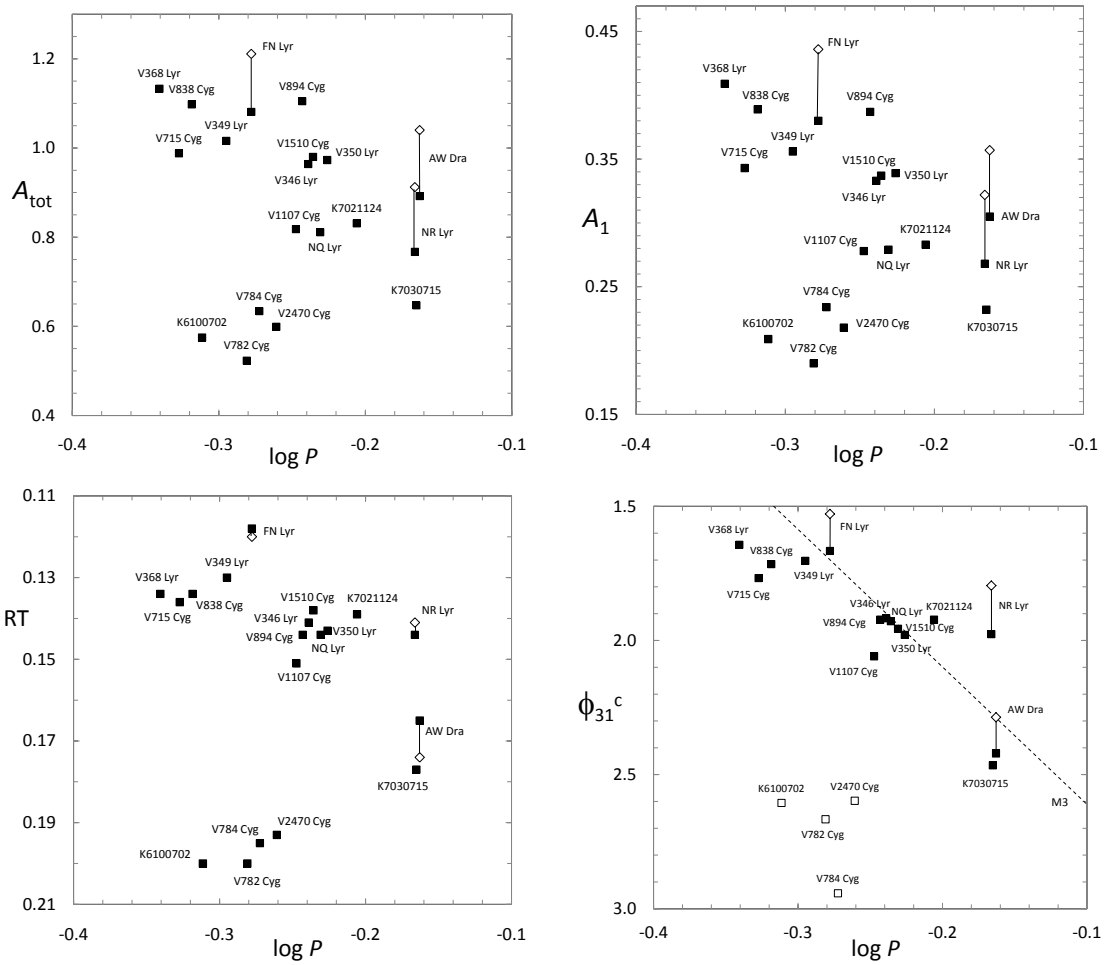

Figure 6.— Period-amplitude and three other metallicity diagnostic diagrams (all with log P along the abscissa) for the *Kepler* non-Blazhko RRab stars. AW Dra, FN Lyr and NR Lyr are plotted twice in each panel: the *Kepler* points are shown as black squares, the V-photometry points are shown as open diamonds, and the two are connected by vertical lines. The consistency of the *Kp*-V offsets seen here and elsewhere justifies using the J98 and Sandage relations to calculate physical characteristics. In the lower-right panel the four metal rich stars have been plotted as open-squares, and the dashed diagonal line is the observed V-relation for the M3 RR Lyrae stars (from Cacciari *et al.* 2005).

Sandage (2006). For the metal-poor stars all three L(evol) are systematically larger than the L(puls) values. For the four metal-rich stars the agreement is better but there is a wide range of L(evol) owing to the linear or non-linear [Fe/H] dependencies. Regardless of which formula was used the most luminous stars have the lowest metallicities and there is internal consistence. It is not clear whether the L(puls) or L(evol) are correct. As was the case for the luminosities, the $\mathcal{M}$(evol) are all larger than the corresponding $\mathcal{M}$(puls) values.

Figure 8 compares the results with the locations of model zero-age horizontal branches and evolutionary tracks. The top two panels show HR diagrams with log $T_{\rm eff}$

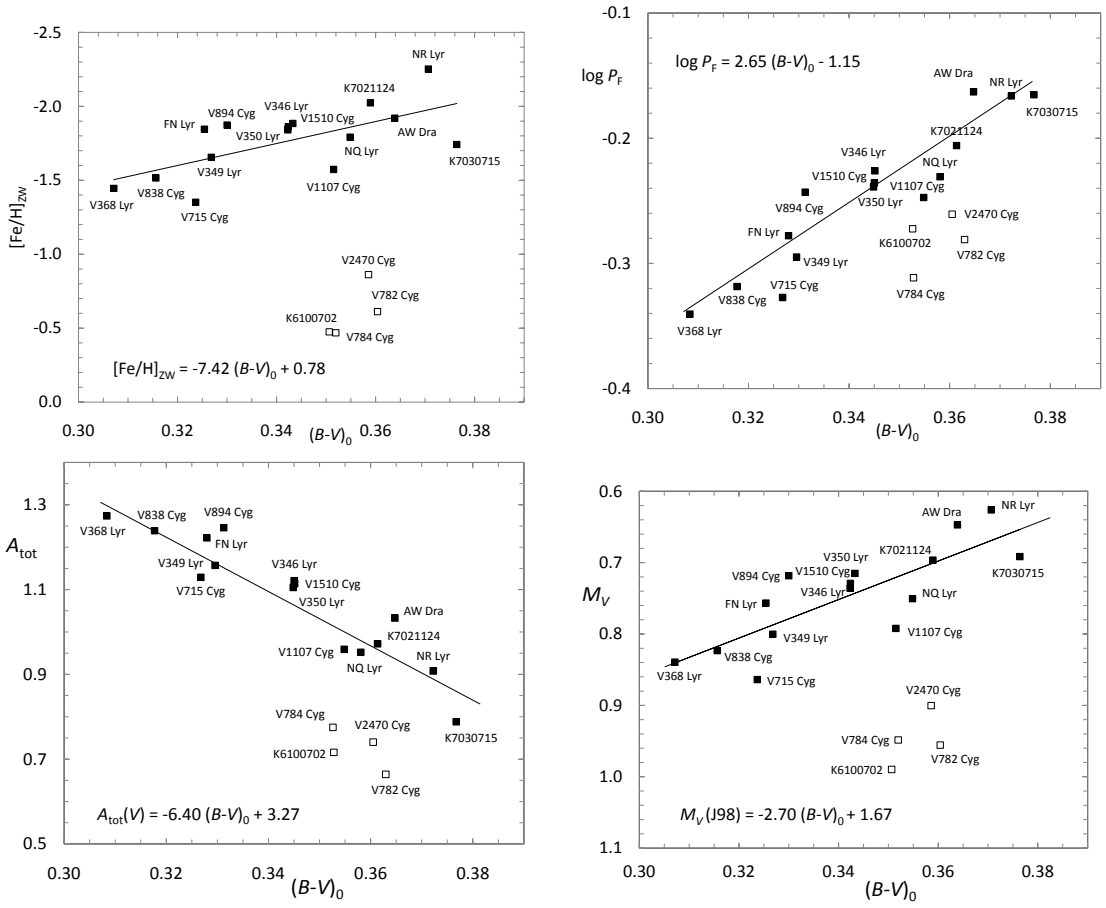

Figure 7.— Four diagrams for the non-Blazhko RR Lyr stars, all with mean dereddened colour $(B-V)_0$ (average of the two values given in column 6 of Table 5) along the abscissa: metallicity *vs.* colour (Top left), period *vs.* colour (Top right), total amplitude *vs.* colour (Bottom left), and absolute magnitude *vs.* colour (Bottom right). In each panel the line (and its equation) is from a least squares fit to the points for the 15 metal-poor stars (*i.e.*, those with [Fe/H]< -1.0 dex).

as abscissa and $\log L$ as ordinate, and two sets of ZAHB loci from Dorman (1992) computed for different masses along the ZAHB. The more luminous horizontal branch assumes [Fe/H]$= -1.78$ dex, and the less luminous branch [Fe/H]$= -0.47$ dex. The numbers next to the symbols are the masses for the individual models, which are seen to be higher for the low-[Fe/H] tracks than for the high-[Fe/H] tracks. For both assumed metallicities oxygen enhanced and non-enhanced ZAHBs have been plotted – the effect of increasing the oxygen to iron ratio from [O/Fe]=0 to 0.66 for the low-metallicity ZAHBs is to lower the luminosity and reduce the mass at a given temperature. For the high-metallicity tracks an oxygen enhancement from [O/Fe]=0 to 0.23 has little effect on the derived L or $\mathcal{M}$. Also plotted in the low-[Fe/H] case are the evolutionary paths away from the ZAHB for two masses, 0.66 and 0.68 $\mathcal{M}_\odot$. In both panels the non-Blazhko RR Lyr stars with low metallicities are represented by large black squares, the

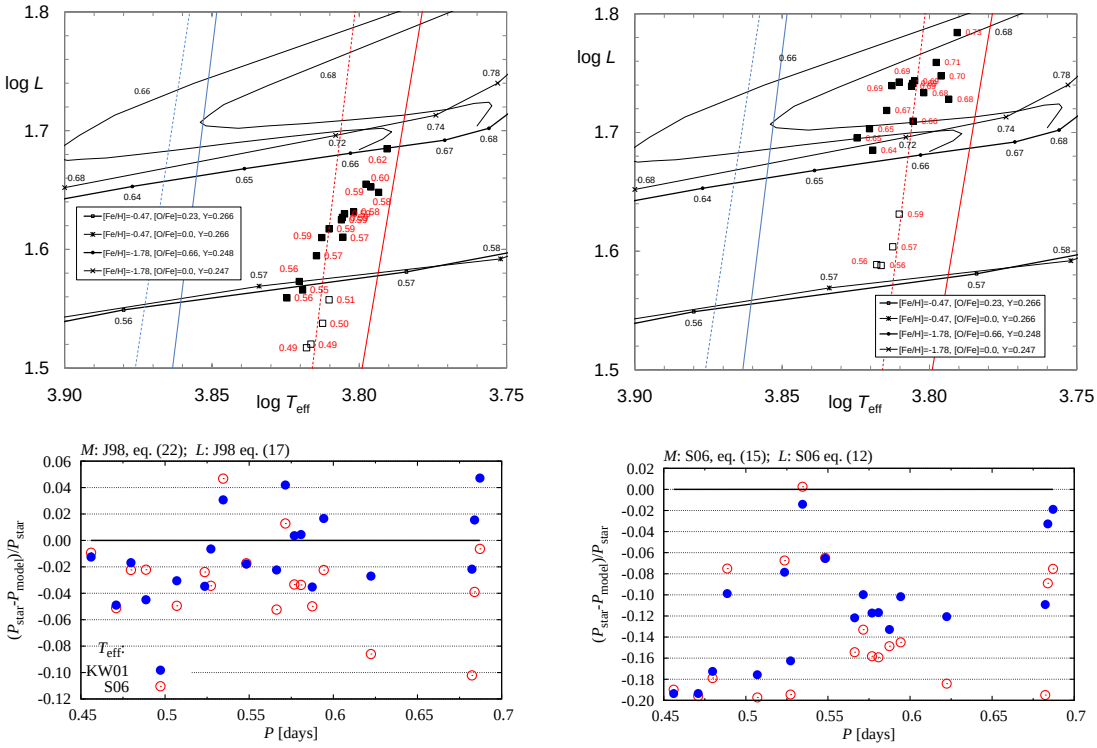

Figure 8.— (**Top panels**) HR-diagrams showing the locations of the *Kepler* non-Blazhko RR Lyr stars compared with two sets of horizontal branch models (low- and high-metallicity) from Dorman (1992). In both graphs the four metal-rich RR Lyr stars have been plotted with open squares and the metal-poor stars with filled squares; the black numbers next to the ZAHB symbols and the two evolutionary tracks are the assumed masses for the individual stellar evolution models. For the non-Blazhko RR Lyr stars in the top left panel the L(puls) were calculated with eq. 17 of J98 and labelled (in red) with the $\mathcal{M}$(puls) calculated with eq. 22 of J98; in the top right panel the L(evol) were calculated with eq. 12 of S06 and labelled (in red) with the $\mathcal{M}$(evol) calculated with eq. 15 of S06. Both panels (left and right) show the blue and red edges for the instability strip computed using the Warsaw pulsation code; the fundamental mode edges are plotted as solid lines, and first-overtone mode edges as dashed lines. (**Bottom panels**) Graphs comparing the observed pulsation periods and the pulsation periods derived with the Warsaw pulsation code. The assumed masses and luminosities are the values given in the top panels. For each star two points are plotted, computed assuming the $T_{\rm eff}$ from eq. 11 of KW01 (blue dots) and from eq. 18 of S06 (red circles). The best agreement is seen in the left panel, with the KW01 temperatures favoured over the S06 values. In both panels the largest differences are seen for the longest period stars, with no metallicity dependence.

four high-metallicity stars are plotted with open squares, and the $T_{\rm eff}$ are the average of the Kovács & Walker (2001, hereafter KW01) and Sandage (2006, hereafter S06) values.

In the top left panel of Fig. 8 the luminosities and masses (labelled in red) of the *Kepler* non-Blazhko RR Lyr stars were calculated with eqs. 17 and 22 of J98 and thus are based on pulsation theory. The L(puls) and $\mathcal{M}$(puls) are seen to be systematically smaller than values derived from the ZAHB tracks (for the appropriate metal abundance). The reddest non-Blazhko RR Lyr stars lie close to the fundamental

mode red-edge and have the smallest amplitudes. This graph also shows blue and red edges of the instability strip for the fundamental mode (red and blue solid lines) and first-overtone mode (red and blue dashed lines). The edges were calculated with the Warsaw pulsation code assuming a mass of 0.65 $\mathcal{M}_{\odot}$. The *Kepler* non-Blazhko stars all lie in the fundamental mode region of the variability strip, and the smallest amplitude RR Lyr stars (the four metal-rich stars, KIC 7030715 and NR Lyr) have locations near the fundamental red edge (FRE) of the instability strip. As expected, all the stars near the FRE have low R_{31} values.

In the top right panel of Fig. 8 the luminosities were calculated with eq. 12 of S06, and the masses (labelled in red) with eq. 15 of S06; thus they are evolutionary L and $\mathcal{M}$ values. In this case there is very good agreement with the stellar evolution models, as one expects since they are based on stellar evolution models. Enhancing the oxygen to iron ratio by the plotted amounts makes little difference.

It is unclear which are correct, the L(puls) and $\mathcal{M}$(puls), or the L(evol) and $\mathcal{M}$(evol). The mass and luminosity discrepancies go in the same direction as seen for Cepheids. Pietrzynski *et al.* (2010) recently derived a dynamical mass $\mathcal{M}$(dynam) for a classical Cepheid in a well detached, double-lined eclipsing binary in the LMC. The mass they derive is very accurate and favours $\mathcal{M}$(puls). The reason for the discrepancies may be the same, as suggested by Pietrzynski *et al.* – not enough mass loss has been taken into account in the evolution models.

Finally, the Nemec *et al.* (2011) paper concludes with a section on hydrodynamic models computed with the Smolec and Moskalik 'Warsaw convective pulsation program'. Perhaps most relevant for the discussion above is the conclusion that in the P-A diagram when [Fe/H] is varied from -0.2 to -1.9 dex there is very little motion at a given amplitude. Instead, motion to longer periods at a given amplitude occurs for stars of higher L for a given mass, or for stars of lower mass for a given luminosity. This suggests that the main factors causing period shifts in the P-A diagram seem to be the mass and luminosity, the latter being caused either by higher ZAHB mass or by post-ZAHB evolution.

5. Conclusions

The main conclusions reached by Nemec *et al.* (2011) concerning the *Kepler* non-Blazhko RR Lyrae stars are: (1) Fourier-based [Fe/H] values have been derived for the stars (using four different correlations), and four of the 19 stars (V782 Cyg, V784 Cyg, KIC 6100702 and V2470 Cyg) appear to be much more metal-rich than the others – recent CFHT spectra confirm that KIC 6100702 is metal-rich with [Fe/H]$= -0.18 \pm 0.06$ dex, and AW Dra is of intermediate metallicity with [Fe/H]$=-1.33 \pm 0.08$) dex. (2) The star KIC 7021124 is found to be doubly-periodic ($P_2/P_0 = 0.59305$) with characteristics similar to V350 Lyr (see Benkő *et al.* 2010); (3) All the stars show remarkably constant light curves ($\sigma < 1$ mmag) over the 420-day interval of the Q0-

Q5 observations; (4) FN Lyr and AW Dra are found to have increasing periods; (5) the ASAS-North photometry of nine of the brightest stars shows that their colours are bluest when brightest, as expected for RR Lyrae stars; (6) Fourier-based physical characteristics for all the stars have been derived; (7) Distances range from 3 to 23 Kpc; (8) Pulsational and evolutionary masses and luminosities are calculated for the stars, the latter tending to be higher in both cases. When the observed periods are compared with periods computed with the Warsaw non-linear convective pulsation code better agreement is achieved assuming *pulsational* L and $\mathcal{M}$ values rather than the (higher) *evolutionary* L and $\mathcal{M}$ values. (9) Finally, the Warsaw models show that varying [Fe/H] has a relatively small effect on the P-A relation and that the main factors causing the period shifts must be luminosity and mass.

6. Acknowledgements

Funding for the *Kepler* Discovery Mission is provided by NASA's Science Mission Directorate. We acknowledge the entire *Kepler* team for their outstanding efforts that have made these results possible. JMN thanks Dr. Andrew McWilliam for the invitation to present these results in Pasadena at such a stimulating conference.

References

Benkő, J.M. *et al.* 2010, MNRAS, 409, 1585
Cacciari, C., Corwin, T.M. & Carney, B.W. 2005, AJ, 129, 267
Dorman, B. 1992, ApJS, 81, 221
Jurcsik, J. 1998, A&A, 33, 571 (J98)
Kolenberg, K. *et al.* 2010, ApJL, 713, 198
Kolenberg, k. *et al.* 2011, MNRAS, 411, 878
Kovács, G. & Walker, A.R. 2001, A&A, 371, 589 (KW01)
Kovács, G. & Kupi, G. 2007 A&A 462, 1007
Lenz, P. & Breger, M. 2005, Comm. in Asteroseismology, 146, 53
Morgan, S., Simet, M. & Bargenquast, S. 1998, Acta Astron. 48, 341
Moskalik, P. *et al.* 2011, in preparation
Nemec, J.M., Walker, A.R. & Jeon, Y.-B. 2009, AJ, 138, 1310
Nemec, J.M., Smolec, R., Benkő, J.M. *et al.* 2011, MNRAS, in press
Pietrzynski, G. *et al.* 2010, Nature, 468, 542
Pigulski, A. et al. 2009, Acta Astron. 59, 33
Sandage, A. 2004, AJ, 128, 858 (S04)
Sandage, A. 2006, AJ, 131, 1750 (S06)
Simon, N. 1988, ApJ, 328, 747
Soszynski, I. *et al.* 2009, Acta Astron. 59, 1
Zinn, R. & West, M.J. 1984, ApJS, 55, 45 (ZW)